

RESEARCH ARTICLE | *Glial Cells and Neuronal Signaling*

# Minocycline blocks glial cell activation and ventilatory acclimatization to hypoxia

 Jennifer A. Stokes, Tara E. Arbogast, Esteban A. Moya, Zhenxing Fu, and Frank L. Powell  
*Division of Physiology, Department of Medicine; University of California, San Diego, La Jolla, California*

Submitted 30 June 2016; accepted in final form 11 January 2017

**Stokes JA, Arbogast TE, Moya EA, Fu Z, Powell FL.** Minocycline blocks glial cell activation and ventilatory acclimatization to hypoxia. *J Neurophysiol* 117: 1625–1635, 2017. First published January 18, 2017; doi:10.1152/jn.00525.2016.—Ventilatory acclimatization to hypoxia (VAH) is the time-dependent increase in ventilation, which persists upon return to normoxia and involves plasticity in both central nervous system respiratory centers and peripheral chemoreceptors. We investigated the role of glial cells in VAH in male Sprague-Dawley rats using minocycline, an antibiotic that inhibits microglia activation and has anti-inflammatory properties, and barometric pressure plethysmography to measure ventilation. Rats received either minocycline (45mg/kg ip daily) or saline beginning 1 day before and during 7 days of chronic hypoxia (CH,  $P_{iO_2} = 70$  Torr). Minocycline had no effect on normoxic control rats or the hypercapnic ventilatory response in CH rats, but minocycline significantly ( $P < 0.001$ ) decreased ventilation during acute hypoxia in CH rats. However, minocycline administration during only the last 3 days of CH did not reverse VAH. Microglia and astrocyte activation in the nucleus tractus solitarius was quantified from 30 min to 7 days of CH. Microglia showed an active morphology (shorter and fewer branches) after 1 h of hypoxia and returned to the control state (longer filaments and extensive branching) after 4 h of CH. Astrocytes increased glial fibrillary acidic protein antibody immunofluorescent intensity, indicating activation, at both 4 and 24 h of CH. Minocycline had no effect on glia in normoxia but significantly decreased microglia activation at 1 h of CH and astrocyte activation at 24 h of CH. These results support a role for glial cells, providing an early signal for the induction but not maintenance of neural plasticity underlying ventilatory acclimatization to hypoxia.

**NEW & NOTEWORTHY** The signals for neural plasticity in medullary respiratory centers underlying ventilatory acclimatization to chronic hypoxia are unknown. We show that chronic hypoxia activates microglia and subsequently astrocytes. Minocycline, an antibiotic that blocks microglial activation and has anti-inflammatory properties, also blocks astrocyte activation in respiratory centers during chronic hypoxia and ventilatory acclimatization. However, minocycline cannot reverse ventilatory acclimatization after it is established. Hence, glial cells may provide signals that initiate but do not sustain ventilatory acclimatization.

astrocytes; hypoxic ventilatory response; microglia; nucleus tractus solitarius; neural plasticity; rat

FOLLOWING EXPOSURE TO CHRONIC SUSTAINED HYPOXIA (CH), an increase in ventilation is observed, which persists even upon return to normoxic conditions, and this is known as ventilatory acclimatization to hypoxia (VAH; Powell et al. 1998). VAH increases  $P_{aO_2}$  and decreases  $P_{aCO_2}$  relative to acute hypoxia by further increasing ventilation resulting from plasticity in 1) peripheral chemoreceptors and 2) brainstem nuclei processing chemoreceptor afferent input. Carotid body peripheral chemoreceptors sense acute changes in  $P_{aO_2}$  and  $P_{aCO_2}$ , but sustained hypoxic exposure increases carotid body  $O_2$  sensitivity (Kumar and Prabhakar 2012). This increases afferent input to the brainstem respiratory center the nucleus tractus solitarius (NTS), and plasticity within the central nervous system (CNS) further increases ventilatory motor output for a given chemoreceptor input (Dwinell and Powell 1999; Pamerter et al. 2014a, 2014b; Pamerter and Powell 2016; Wilkinson et al. 2010). The mechanisms of such plasticity in the NTS involve glutamatergic neurotransmission (Pamerter et al. 2014a, 2014b), but the signals for this plasticity are unknown. It is clear from the literature that glial cells influence neuronal transmission and central respiratory control (Erlichman et al. 2010; Fukushi et al. 2016; Funk et al. 2015; Hülsmann et al. 2000; Huxtable et al. 2010; Lorea-Hernández et al. 2016) and thus may be important in the signaling cascade leading to acclimatization.

Glial cells present in brainstem respiratory centers surround the neural synapses and neighboring blood vessels and are critical players in neuronal signaling and synaptic transmission (Bezzi and Volterra 2001). Glial cells can be activated by neurotransmitter release and, in turn, release their own gliotransmitters modulating synaptic transmission (Accorsi-Mendonça et al. 2013). Astrocytes are a heterogeneous population of glial cells that regulate neurotransmitter availability in the synapse, and some are chemosensitive (Gourine et al. 2010; Panatier et al. 2011; Vesce et al. 1999). Microglia are thought to be upstream of astrocytes in that, upon activation by neurotransmitters, microglia release small amounts of ATP, activating neighboring astrocytes, which then amplify neuronal signaling (Pascual et al. 2012). In respiratory centers of the brainstem, both microglia and astrocytes appear to be activated by sustained hypoxia as shown by immunofluorescent staining (Tadmouri et al. 2014). Inhibiting microglia activation with minocycline inhibits VAH after 24 h of sustained hypoxia, as well as astrocyte activation, further supporting the idea that astrocyte activation is modulated by microglial activation

Address for reprint requests and other correspondence: J. Stokes, Division of Physiology, Dept. of Medicine; University of California, San Diego; 9500 Gilman Dr., MC 0623A, La Jolla, CA 92032-0623A (e-mail: jenniferstokes@gmail.com).

(Tadmouri et al. 2014). The studies presented here tested the hypothesis that microglia activation is a critical signal for ventilatory acclimatization to sustained hypoxia, and this precedes astrocyte activation in the NTS.

## MATERIALS AND METHODS

**Animals.** All animal experiments were carried out according to protocols approved by the Institutional Animal Care and Use Committee of the University of California, San Diego (under the *Guide for Care and Use of Laboratory Animals*; publication 85-23; NIH, Bethesda, MD). Adult, male Sprague-Dawley rats (~10 wk of age; 250–300 g; Harlan/Envigo) were housed up to three per standard cage at room temperature, maintained on a 12-h:12-h light/dark cycle. Testing was performed during the light cycle. Food and water were available ad libitum except when animals were in the plethysmograph to measure ventilation.

**Experimental groups and minocycline administration.** Two studies were designed to assess effects of minocycline, an antibiotic and putative microglia inhibitor, on ventilation during exposure to CH or normoxia (CN). Minocycline (Sigma-Aldrich; M9511), a tetracycline derivative antibiotic, is commonly used to suppress microglia activation (Blackbeard et al. 2007; Lorea-Hernández et al. 2016; MacFarlane et al. 2016; Tadmouri et al. 2014). Ventilation *study 1* consisted of four groups of rats ( $n = 3$  rats/group) under the following individual conditions: CN-saline, CN-minocycline, CH-saline, or CH-minocycline. CH exposure for *study 1* was 7 days in a hypobaric chamber (barometric pressure = 380 Torr,  $P_{\text{I}_2\text{O}_2} = 70$  Torr,  $[\text{O}_2] = 10\%$ , temperature = 21°C with 40% relative humidity). Rats received one prehypoxia dose of either saline or minocycline (45 mg/kg ip) followed by daily doses of saline or minocycline (45 mg/kg ip) each day in the hypobaric chamber, or in normoxia. At the end of the 7-day hypoxia exposure time course, rats were placed in a whole body plethysmograph for ventilation recordings. In ventilation *study 2* rats were exposed to 7 days of hypoxia and administered minocycline (45 mg/kg ip) in one of two regimes: *Early* minocycline, minocycline *days 0–3* of hypoxia exposure and saline *days 4–7*; and *Late* minocycline, saline *days 0–3* of hypoxia and minocycline *days 4–7* ( $n = 3$  rats/group). Ventilation was recorded using whole body plethysmography on *day 4* (before treatment change) and on *day 7*, after the final hypoxic day. The final minocycline or saline dose was administered at the start of the last 24 h in the chamber, for both ventilation *study 1* and ventilation *study 2*.

To obtain the time course of glial cell activation with varying lengths of CH, rats ( $n = 3–4$ /group) were exposed to CH and euthanized for immunohistochemical or morphometric analysis at the following time points: 30 min, 1 h, 4 h, 24 h, 4 days, and 7 days (Figs. 3 and 4). For shorter time points of 4 h or less, rats were placed in a chamber with constant airflow maintained at 10%  $\text{O}_2$ . For hypoxic exposure of over 24 h or more, we used a hypobaric chamber as described previously (Pamenter et al. 2014a, 2014b). The chamber was held at half the normal sea level barometric pressure (barometric pressure = 380 Torr,  $P_{\text{I}_2\text{O}_2} = 70$  Torr) and other environmental conditions inside comparable to those in the vivarium, laboratory, or plethysmograph (temperature = 21°C with 40% relative humidity).

An additional minocycline administration study was set up to assess the effect of minocycline (45 mg/kg ip) on glial cell activation in respiratory centers during CH (Fig. 5). We studied the following nine groups of rats ( $n = 3–6$ /group): normoxia, normoxia + saline, normoxia + minocycline, 1 h CH, 1 h CH + saline, 1 h CH + minocycline, 24 h CH, 24 h CH + saline, and 24 h CH + minocycline. Animals were euthanized, and tissue was processed for immunohistochemistry and morphometric analysis as described below in *Immunofluorescent labeling of brainstem microglia and astrocytes*.

**Plethysmography.** Ventilatory responses to hypoxia and hypercapnia were measured in unrestrained rats using a whole body barometric plethysmograph (7 l) modified for continuous flow (Pamenter et al.

2014a; Reid and Powell 2005). Briefly, flow was maintained constant through the chamber while a pressure transducer (mMP45 with 2 cmH<sub>2</sub>O diaphragm, Validyne) recorded the changes attributable to the warming and expansion of inhaled gases.

On the experimental day, the rats were weighed and sealed into the plethysmograph chamber along with a temperature and humidity probe (Thermalert TH5, Physitemp). A constant gas flow (3 l/min) was delivered with a mass flow controller and gas mixer (MFC-4 Sable Systems) upstream of the chamber. Gases exited the chamber through a valve and into a vacuum pump (Model 25, Precision Scientific) to isolate pressure changes from breathing in the chamber during constant flow with high input and output impedances. This also allows us to maintain chamber pressure near-atmospheric pressure and reference pressure measurements (Validyne) in the chamber to atmosphere. Inspired and expired oxygen and carbon dioxide fractions were measured with an  $\text{O}_2/\text{CO}_2$  mass spectrometer (RAMS M-100; GE Marquette Medical Systems) sampling from the chamber.

**Data acquisition and analysis.** All ventilatory parameters were recorded on an analog-digital acquisition system (PowerLab 8SP, AD Instruments) and analyzed with the LabChart 8-Pro Software, sampling at a rate of 1 kHz. We analyzed a minimum of 30 s as part of the region of interest between 10 and 15 min after changing gas concentrations. The frequency (breaths/min) and tidal volume (ml) were calculated from cyclic peaks in the plethysmograph pressure pulses, and tidal volume was measured using 0.2-ml calibration pulses; the equations were developed by (Drorbaugh and Fenn 1955). The product of frequency and tidal volume is inspired ventilation ( $V_i$ ), which was normalized to body mass ventilation (ml/min·kg).

**Immunofluorescent labeling of brainstem microglia and astrocytes.** At the end of the specified time point, rats were first anesthetized (Fatal Plus, Vortech, 150 mg/kg ip) to a deep surgical plane confirmed by lack of response to a toe pinch. Animal tissues were fixed via transcardial perfusion, first flushed with 0.9% saline/0.004% heparin, followed by 4% paraformaldehyde (PFA). The brainstem was removed and postfixed in 4% PFA overnight followed by immersion in 30% sucrose. Brainstem tissue was mounted and frozen in optimal cutting temperature compound (Tissue-Tek, Sakura) and sectioned on a Leica cryostat in 40- $\mu\text{M}$  sections. For labeling with antibodies against ionized calcium binding adaptor molecule 1 (Iba-1; microglia) and glial fibrillary acidic protein (GFAP; astrocytes), sections were incubated at 4°C for 2 days in a solution of PBS with 0.1% Triton, 1% normal goat serum, Iba-1 (rabbit; 1:2,000; Wako), and GFAP (chicken; 1:2,000; Life Technologies). After the 2-day primary incubation, sections were rinsed in PBS and incubated for 1 h at room temperature with secondary antibodies Cy3-goat-anti-rabbit (1:1,000; Jackson ImmunoResearch) and 488-goat-anti-chicken (1:500; Life Technologies). Sections were mounted on slides and coverslipped with ProLong Diamond anti-fade with DAPI. Images were acquired using a Leica SP5 confocal system.

**Quantifying microglia activation.** We used IMARIS software (Bitplane, Oxford Instruments, v. 8.2) to quantify changes in microglia morphology as measures of activation (Fontainhas et al. 2011; Morrison and Filosa 2013). Experimental groups were coded and blinded during quantification to prevent investigator bias. Using the IMARIS FilamentTracer, microglia cell bodies and branches were semiautomatically traced through the three-dimensional plane of the confocal  $z$ -stack image. This tracing created a filament skeleton overlaying the immunofluorescent Iba-1 antibody labeling microglia (see Fig. 3). The NTS region was selected from the image and parameters to assess microglia activation, including the average length of branches per microglia and the average number of end points per microglia. Microglia cell count was included in this analysis.

Selection of the NTS region was based on identification of the central canal and area postrema. A rectangular region lateral to the central canal and inferior to the area postrema was selected for each individual image (see Figs. 3 and 4 for schematics). The total area selected was the same for every image.

**Quantifying astrocyte activation.** We quantified astrocyte activation as mean GFAP immunofluorescent intensity using ImageJ (FIJI; software v. 2.0.0) freely available by the NIH. This approach is based on previous work showing that astrocytes upregulate GFAP protein during activation (Eng and Ghirnikar 1994). Experimental groups were coded and blinded during quantification to prevent investigator bias. We used the Analyze-Measure tool in FIJI to analyze the mean fluorescence intensity of the GFAP-positive area within the selected NTS region. All images were background corrected based on their own fluorescent staining by subtracting the background region of the individual image from the GFAP-positive selection. To address the question of astrocyte proliferation, an astrocyte count was performed with a colocalization cell count of GFAP and DAPI.

**Statistics.** All statistics are based on raw data values, and all data are presented as means  $\pm$  SE. All statistical analysis was performed using PRISM software (Graphpad Software, v. 5.0d). Ventilation data sets were analyzed by two-way ANOVA with Bonferroni posttest. Astrocyte and microglia activation across CH time points were analyzed by one-way ANOVA with Dunnett's posttest. Two-way ANOVA with Bonferroni posttest was used to assess the effects of intraperitoneal saline and intraperitoneal minocycline on glial cell activation in normoxia, 1 h of hypoxia, and 24 h of hypoxia, and a one-way ANOVA with Bonferroni multiple-comparisons posttest was used to assess effects of CH alone. Statistical tests, *P* values, and symbols are noted in each figure legend.

## RESULTS

**Minocycline administration blocks VAH.** Ventilation increased in chronically hypoxic rats compared with normoxic control rats treated with saline (Fig. 1A), similar to previous reports from our laboratory (e.g., Pamerter et al. 2014a; 2014b). Minocycline administered to rats during a 7-day CH exposure significantly ( $P < 0.001$ ) decreased ventilation in hypoxia, so it was no different than normoxic control rats (Fig. 1A; at 10% inspired  $O_2$  hypoxia-saline  $\dot{V}_I = 2188.0 \pm 51.3$  ml/min·kg, hypoxia-minocycline  $\dot{V}_I = 1397.7 \pm 147.7$  ml/min·kg, normoxia-saline  $\dot{V}_I = 1249.7 \pm 36.4$  ml/min·kg, nor-

moxia-minocycline  $\dot{V}_I = 1255.8 \pm 17.3$  ml/min·kg) while having no effect on the hypercapnic ventilatory response (Fig. 1B). Minocycline also had no effect on normoxic animals treated for 7 days (Fig. 1, A and B), thus there are no effects of minocycline on ventilation in the absence of CH. In examination of the pattern of breathing, minocycline significantly ( $P < 0.001$ ) decreased frequency (Fig. 1C; at 10% inspired  $O_2$  hypoxia-saline  $190.0 \pm 4.2$  breaths/min, hypoxia-minocycline  $133.3 \pm 1.3$  breaths/min, normoxia-saline  $128.9 \pm 4.8$  breaths/min, normoxia-minocycline  $116.8 \pm 11.9$  breaths/min), with no effect on tidal volume (Fig. 1D) after 7 days of CH.

**Early microglia activation required for VAH.** To determine whether minocycline exerts an effect on VAH at specific times during CH, we administered minocycline either *Early* or *Late* during 7 days of CH. *Early* minocycline administration for the first 3 days of CH blocked the increase in ventilation ( $P < 0.05$ ) in hypoxia on *day 4*; note in Fig. 2A,  $\dot{V}_I$  breathing 10%  $O_2$  after *Early* minocycline ( $\square$ , dashed line; at 10% inspired  $O_2$   $\dot{V}_I = 1459.1 \pm 158.0$  ml/min·kg) is not significantly greater than in a normoxic control rat illustrated with the thin solid gray line ( $\dot{V}_I = 1249.7 \pm 36.4$  ml/min·kg). However, stopping minocycline treatment during *days 5 to 7* of CH allowed ventilatory acclimatization to proceed with increased ventilation in normoxia and hypoxia on *day 7* (Fig. 2A,  $\blacksquare$ , solid line; at 10% inspired  $O_2$   $\dot{V}_I = 1678.1 \pm 99.4$  ml/min·kg).

In contrast, *Late* minocycline administration during *days 4–7* of CH was not able to reverse VAH (Fig. 2D). There was no difference between the elevated levels of ventilation relative to normoxic controls (thin line in Fig. 2D) after 4 days of saline (Fig. 2D,  $\circ$ , dashed line) vs. minocycline during *days 5 to 7* (Fig. 2D,  $\bullet$ , solid line).

The effects of minocycline on ventilation are explained mainly by changes in breathing frequency (Fig. 2, B and E), whereas tidal volume was not affected (Fig. 2, C and F). *Early* minocycline resulted in lower breathing frequency ( $P < 0.01$ ) after 4 days of CH relative to the value reached after saline

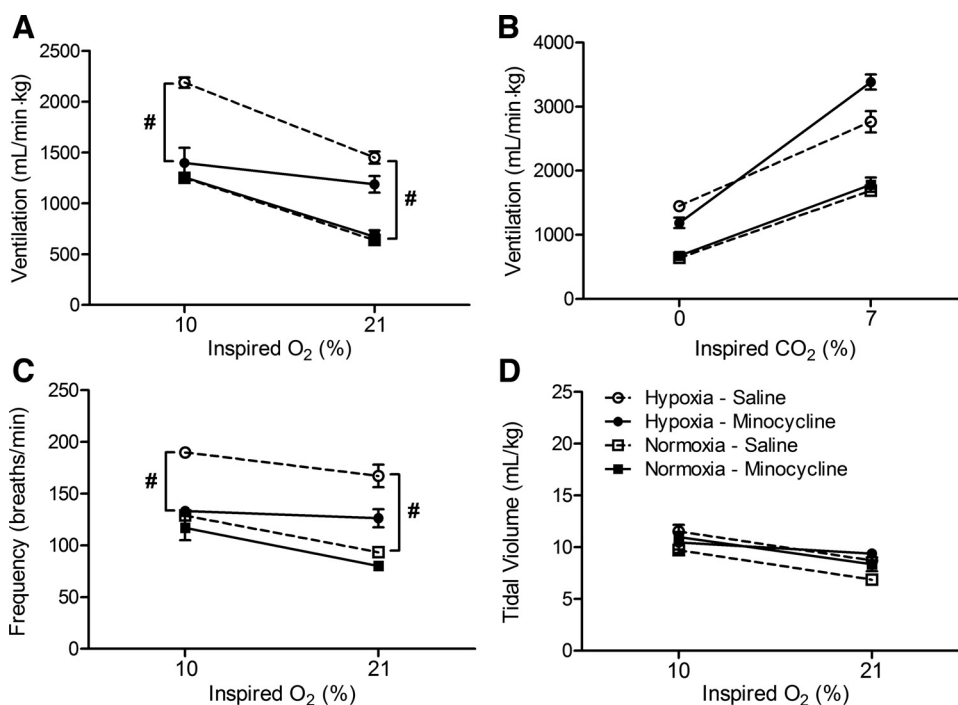


Fig. 1. Systemic minocycline administration blocks ventilatory acclimatization to hypoxia (VAH) in 7-day chronic sustained hypoxia (CH). Following exposure to 7 days of CH, ventilation significantly increased in saline-treated rats compared with saline-treated normoxic control rats (A). Minocycline administration significantly blocked VAH in CH with no effect on ventilation in the minocycline-treated normoxic control rats (A), and no effect of minocycline was observed in the hypercapnic ventilatory response (B). Minocycline administration blocked the hypoxia-induced increase in breathing frequency with CH (C), with no effect on tidal volume (D). All data are presented as means  $\pm$  SE,  $n = 3-4$  animals/group; # $P < 0.001$ , 2-way ANOVA across groups (normoxic-saline vs. hypoxic-saline, and hypoxic-saline vs. hypoxic-minocycline).

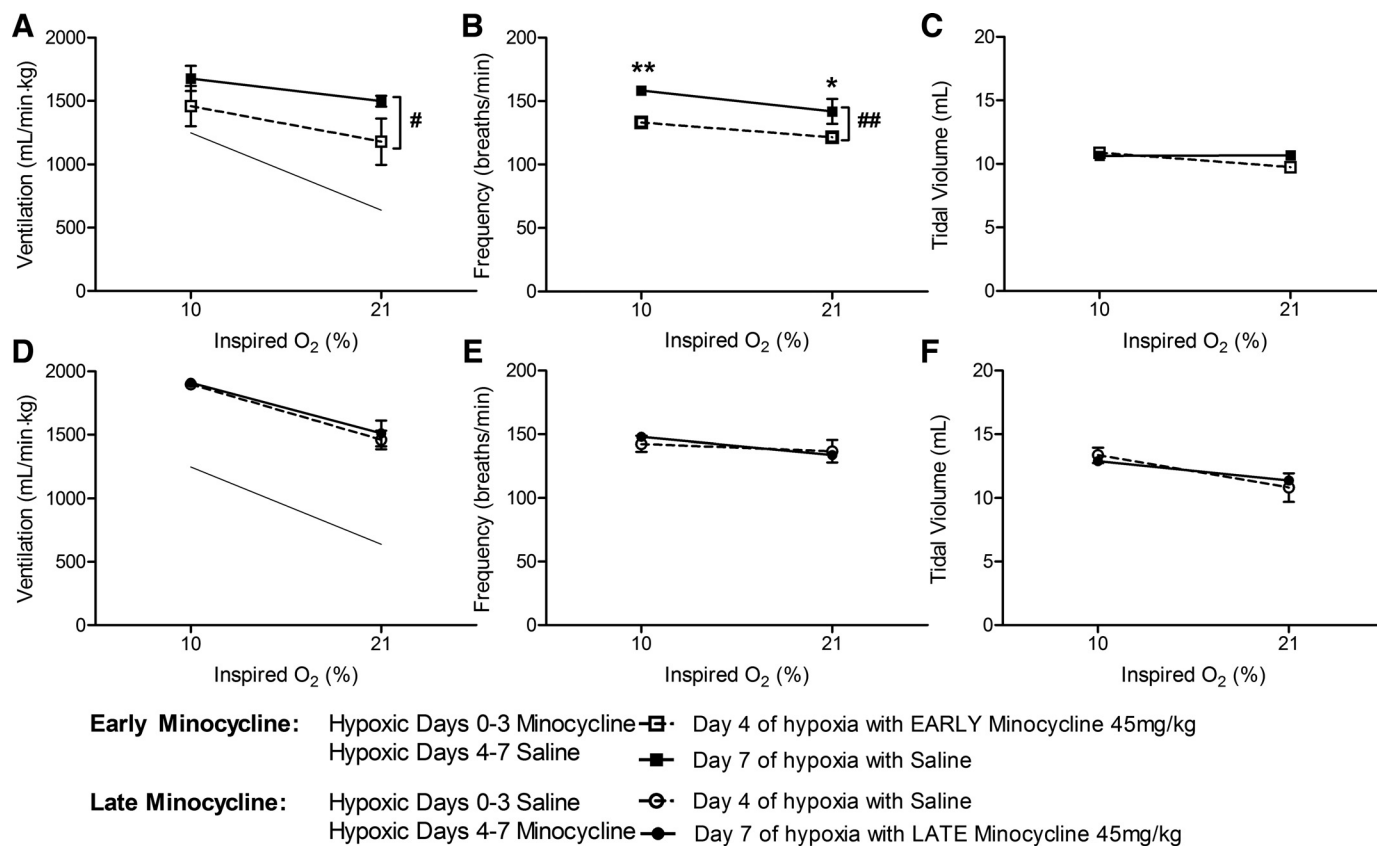


Fig. 2. Minocycline blocks the initiation but not maintenance of VAH. *Early* minocycline administration initially blocked VAH on *day 4*, but, after saline administration during the final days of hypoxic exposure, ventilation increased (A), which was a frequency-dependent effect (B), with no effect on tidal volume (C). *Late* minocycline administration had no effect on ventilation (D), breathing frequency (E), or tidal volume (F) after VAH was already established. Thin solid lines (A and D) show data from normoxic rats (from Fig. 1) for comparison. All data are presented as means  $\pm$  SE,  $n = 3$  animals/group; # $P < 0.05$ , ## $P < 0.01$ , 2-way ANOVA across groups; \* $P < 0.05$ , \*\* $P < 0.01$ , 2-way ANOVA with Bonferroni posttest comparing inspired  $O_2\%$ .

treatment for *days 4–7* of CH (Fig. 2B,  $133.0 \pm 2.6$  breaths/min vs.  $158.5 \pm 3.5$  breaths/min at 10% inspired  $O_2$ ). There were no differences in breathing frequency of tidal volume with *Late* minocycline treatment, consistent with no differences in ventilation (Fig. 2, D–F). These results are consistent with a minocycline-sensitive signal initiating the plasticity involved in acclimatization, but, once acclimatization is established, blocking the signal does not reverse it.

**Microglia and astrocyte activation time course during CH.** The effect of *Early* minocycline administration on VAH and the lack of a reversal effect on established VAH with *Late* minocycline administration led us to investigate the timeline of microglia and astrocyte activation in the NTS with sustained hypoxia. To measure the time course of microglia activation, we quantified the change in microglia morphology from a ramified (resting) state to an amoeboid (activated) state by measuring two parameters: 1) the average branch length per microglia and 2) the average number of end points per microglia. The NTS region of interest for analysis is outlined with the dashed white rectangle in Fig. 3A. Figure 3B shows how we measured branch length (red lines) from the soma (blue circle) to end points (green circles), and example skeletons are superimposed on the bottom two images of Fig. 3C. We compared both parameters across different time points of CH exposure and observed a significant ( $P < 0.01$ ) shift in microglia morphology indicative of activation at 1 h of CH, with a decrease in the branch length (Fig. 3D; normoxia  $169.8 \pm 22.1$

$\mu\text{m}$ ; 1 h CH  $107.3 \pm 10.9 \mu\text{m}$ ) and decrease in the number of end points (Fig. 3E; normoxia  $11.9 \pm 1.7$ ; 1 h CH  $7.2 \pm 0.8$ ). A return to a ramified state indicative of resting microglia was seen by 24 h of CH (Fig. 3D), when there was a significant overshoot ( $P < 0.05$ ) in the number of end points (Fig. 3E; normoxia  $11.9 \pm 1.7$ ; 24 h CH  $15.6 \pm 1.1$ ), but this returned to baseline by 4 days also. The number of microglia did not change over 7 days of CH (Fig. 3F).

Astrocyte activation was quantified by measuring the average mean fluorescence intensity of GFAP protein in the NTS (Fig. 4). The NTS region of interest is outlined with a white dashed rectangle in Fig. 4A, and representative images from selected time points are shown in Fig. 4B. Astrocyte activation peaked ( $P < 0.05$ ) at 4–24 h of CH but decreased and was not significantly different from normoxia at 4–7 days (Fig. 4C; normoxia  $6.0 \pm 0.8$ ; 4 h CH  $9.3 \pm 1.7$ ; 24 h CH  $9.7 \pm 1.3$ ). The number of astrocytes did not change throughout CH exposure (Fig. 4D). Summarizing, microglia are activated before astrocytes by CH, and both types of glia return to control states by 4–7 days of CH when acclimatization occurs.

**Minocycline inhibits glial cell activation in the NTS.** Given the differences in microglia and astrocyte activation over 1–24 h of sustained hypoxia (Figs. 3 and 4), we tested the effects of minocycline on microglia and astrocyte activation by CH during this period. We chose 1 h of CH as the peak of microglia activation with no change in astrocytes and 24 h as

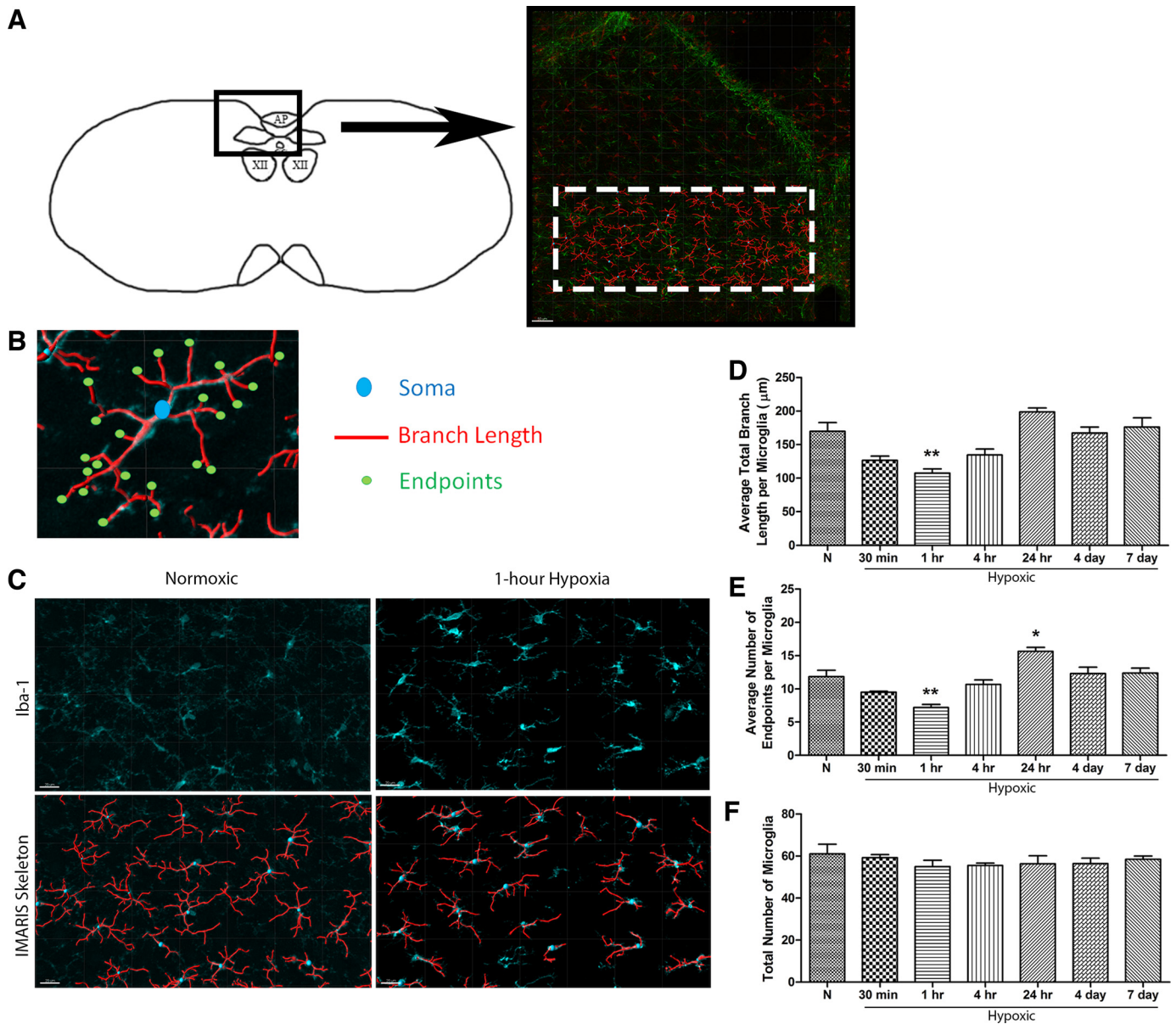


Fig. 3. Quantifying changes in microglia morphology in the rat nucleus tractus solitarius (NTS) during sustained hypoxia. IMARIS software was used to trace a skeleton of microglia filaments through the selected NTS region (white dashed outline), z-stack confocal image (A). The average branch length per microglia (tracing the red skeleton from the blue soma to green end point) and average number of end points per microglia (green circles) (B) are shown. C: examples of tracings include the following: *top*: z-stack confocal image of blue immunofluorescent staining of microglia labeled with Iba-1. *Bottom*: IMARIS red skeleton overlaying the blue fluorescent staining. Scale bar = 20  $\mu\text{m}$  in all 4 images. After 1 h of hypoxia, the microglia have shorter branches (D) and a decrease in end points (E) in the NTS. The number of microglia remained constant throughout the time points of hypoxia exposure (F);  $n = 3\text{--}4$  animals/group; 1-way ANOVA with Dunnett's posttest; \* $P < 0.05$ ; \*\* $P < 0.01$ .

a time when astrocytes were activated but microglia had returned to control. Figure 5, A and B, shows microglia changing to an activated shape with 1 h of CH (similar to Fig. 3), but this is blocked by minocycline. At 1 h of CH, minocycline administration blocked the decrease in branch length (Fig. 5A;  $P < 0.001$ ; 1 h CH no treatment  $143.9 \pm 17.8 \mu\text{m}$ ; 1 h CH saline  $142.2 \pm 6.4 \mu\text{m}$ ; 1 h CH minocycline  $188.6 \pm 18.7 \mu\text{m}$ ) and number of end points (Fig. 5B;  $P < 0.01$ ; 1 h CH no treatment  $9.9 \pm 1.3$ ; 1 h CH saline  $10.3 \pm 1.3$ ; 1 h CH minocycline  $13.6 \pm 1.5$ ) to more closely resemble the normoxic animal values (branch length: normoxia no treatment  $216.8 \pm 13.0 \mu\text{m}$ ; normoxia saline  $225.6 \pm 10.5 \mu\text{m}$ ; normoxia minocycline  $208.8 \pm 27.5 \mu\text{m}$ ; and number of end

points: normoxia no treatment  $15.7 \pm 1.6$ ; normoxia saline  $17.0 \pm 0.6$ ; normoxia minocycline  $14.9 \pm 2.8$ ). No effect of minocycline was observed at 24 h of CH, when microglia are no longer in their "active" amoeboid shape (Fig. 5, A and B), and minocycline had no effect on microglia number at 1 h of hypoxia (saline =  $50.330 \pm 4.933$ , minocycline =  $47.330 \pm 6.110$ ) or 24 h of hypoxia (saline =  $42.670 \pm 4.726$ , minocycline =  $43.330 \pm 5.033$ ) compared with normoxic control ( $43.670 \pm 3.512$ ).

Minocycline also significantly ( $P < 0.001$ ) inhibited astrocyte activation at 24 h of CH and even significantly ( $P < 0.05$ ) reduced GFAP expression relative to normoxic values at 1 h of hypoxia (Fig. 5C; relative GFAP intensity values at 1 h CH

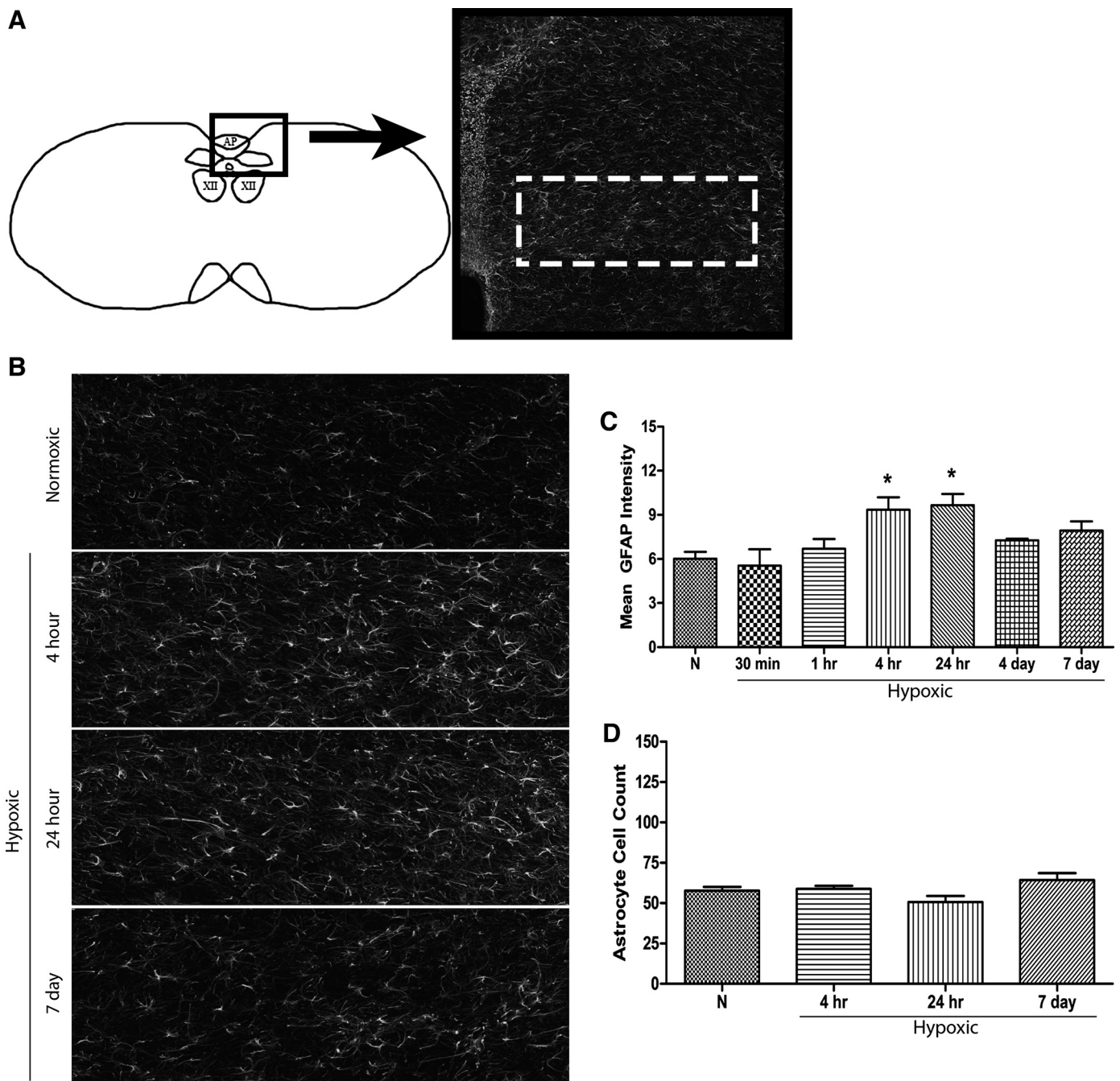


Fig. 4. Astrocyte activation quantification in the rat NTS following sustained hypoxia. Astrocyte activation was assessed in the NTS region outlined by the white-dashed rectangle (A). The mean glial fibrillary acidic protein (GFAP) antibody intensity increased after 4 h and remained elevated at 24 h of sustained hypoxia exposure in the NTS (B and C). The number of astrocytes did not change throughout selected time points of interest in the NTS (D);  $n = 3-4$  animals/group; 1-way ANOVA with Dunnett's posttest;  $*P < 0.05$ .

saline  $1.20 \pm 0.16$ ; 1 h CH minocycline  $0.91 \pm 0.12$ ; 24 h CH saline  $1.30 \pm 0.15$ ; 24 h CH minocycline  $0.76 \pm 0.02$ ). These results are consistent with microglia in the NTS responding to CH before astrocytes and microglial activation providing a signal for astrocyte activation.

#### DISCUSSION

The presented results show the following: 1) glial cell activation in the NTS, which is an important medullary respiratory center, occurs during the first hours to day of chronic

hypoxia; 2) VAH does not occur when microglia and astrocyte activation is blocked by minocycline, during *Early* exposure to CH; 3) minocycline administered after 4 days of CH does not reverse VAH; and 4) microglia activation in sustained hypoxia precedes astrocyte activation, and astrocytes are not activated when microglia activation is blocked by minocycline. Together these data support a working model for ventilatory acclimatization that requires early microglia and then astrocyte activation by sustained hypoxia to initiate neural plasticity in brainstem respiratory centers.

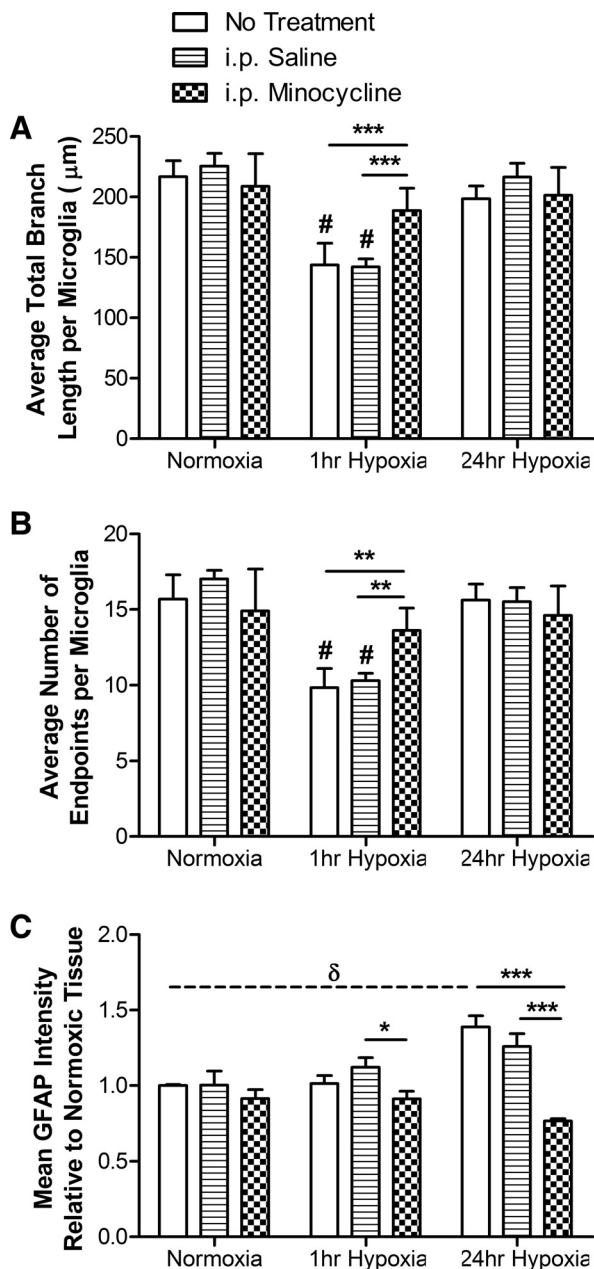


Fig. 5. Minocycline inhibits microglia and astrocyte activation in CH. Microglia morphology and astrocyte activation was assessed in the NTS region at 1 h and 24 h of CH with either saline or minocycline. Normoxic animals with either intraperitoneal saline or minocycline are presented as controls. Following 1 h of CH, microglia displayed a more amoeboid shape with shorter (A) and fewer branches (B), and minocycline administration blocked this morphology shift with branch length and number of endpoints more closely resembling the normoxic animal values. Minocycline also significantly inhibited astrocyte activation at 24 h of CH and at the 1 h CH time point (C);  $n = 3-6$  animals/group; 2-way ANOVA comparing treatments;  $*P < 0.05$ ;  $**P < 0.01$ ;  $***P < 0.001$ . 1-way ANOVA with Bonferroni multiple-comparisons posttest to compare normoxia vs. hypoxic conditions;  $\#P < 0.001$  and  $\delta P < 0.05$ .

**Glia and central respiratory control.** The data presented here add to the evolving story of glial cell involvement of respiratory control and VAH. In the present study, minocycline administered to rats during a 7-day CH exposure significantly decreased ventilation in hypoxia, mainly by an effect on breathing frequency, but it did not depress the persistent hyperventilation when normoxia is restored acutely. We also

show that, once VAH is established, glial cell inhibition by minocycline cannot reverse VAH, suggesting that glia are involved in the early steps of neural plasticity that develops in the NTS with CH. This is consistent also with neurophysiological measurements indicating that an increase in firing of NTS neurons following 24 h of CH is mediated by glial cells (Accorsi-Mendonça et al. 2015).

The NTS serves as an integration center for peripheral chemoreceptor primary afferents and second-order neurons, sending projections to other brain regions contributing to respiratory control in hypoxia (Accorsi-Mendonça and Machado 2013; Chitravanshi and Sapru 1995; Donoghue et al. 1984; Mifflin 1992). Thus activation of glia in the NTS by primary afferents from the carotid body could have profound effects on ventilatory control. Astrocytes have already been shown as key mediators in peripheral chemoreflex pathways (Accorsi-Mendonça et al. 2013; Lin et al. 2013), and both microglia and astrocytes are activated in the NTS in CH (Tadmouri et al. 2014). Additionally, astrocytes present in brainstem chemosensitive areas release ATP in response to physiological decreases in pH (Gourine et al. 2010). Given the very pronounced presence and activity of glial cells in the chemical control of ventilation, we propose that it will be productive to investigate other well-known functions of glia in neural plasticity of chemoreflexes, such as new synapse connections or synaptic pruning of overactive neurons (Allen 2014; Ji et al. 2013; Kettenmann et al. 2013).

**Microglia and astrocyte activation timeline in hypoxia.** Given previous reports of different times for activation of astrocytes vs. microglia in the NTS during 24 h of hypoxia and the effect of minocycline to block increases in the hypoxic ventilatory response (HVR) between 6 and 24 h of hypoxia (Tadmouri et al. 2014), we hypothesized that the sequence of glial activation in the NTS is important for VAH. Tadmouri et al. (2014) found astrocyte activation first at 1 h of CH, followed by microglia activation at 6 h. In contrast, using a morphology-based method for quantifying microglial activation, we found that microglia were activated before astrocytes during the first hours of sustained hypoxia, and with days of hypoxia both types of glia return to control states when acclimatization occurred. Tadmouri et al. (2014) used an increase in colocalization of Iba-1 and CD11b as a marker of microglia activation. This is based on the observation that microglia increase their cell surface expression of CD11b via reactive oxygen species in neuroinflammatory disease states (Roy et al. 2008). However, CD11b is also detected in “resting” microglia (González-Scarano and Baltuch 1999), so colocalization with Iba-1 does not necessarily indicate activation. Also, as discussed in more detail below, newer evidence supports the view that microglia are never resting but rather they have different functions associated with their morphology; thus the morphological assessment of activation we used should be more accurate than immunohistochemistry alone.

In the time course of NTS microglia and astrocyte activation illustrated in Figs. 3 and 4, the first activation response is in microglia as they shift from a ramified, extended branching form to an amoeboid morphology. In a ramified state, the extended microglia processes are continually retracting and expanding to survey their surrounding environment (Hanisch and Kettenmann 2007; Nimmerjahn et al. 2005; Tremblay et al. 2011). When microglia react to extracellular signals, they

change morphology to an amoeboid, reactive form (Kreutzberg 1996), where they can take on many roles, including release of cytokines or other gliotransmitters, or phagocytose apoptotic cells (Hanisch and Kettenmann 2007). Microglia can release small amounts of ATP, which binds to P2Y1R on astrocytes, which can then lead to amplification of ATP release by astrocytes (Pascual et al. 2012), further propagating the initial neuronal stimuli. In accordance with previous reports (Tadmouri et al. 2014), we also found that minocycline administration inhibited both microglia and astrocytes, suggesting cross-talk between the two types of glia when activated by hypoxia.

One additional finding of note in this study was the significant increase in the number of microglia end points after 24 h of hypoxia compared with normoxic control, as they recovered from the ramified and activated state at 4 h of hypoxia (Fig. 3D). We speculate that this could be due to higher levels of ATP in the extracellular space subsequent to astrocyte activation or an increase in neuronal activation, as ATP has been shown to promote increased branching and heightened surveillance by microglia (Dissing-Olesen et al. 2014). Microglia distribution is heterogeneous (Lawson et al. 1990), and their phenotypic heterogeneity is related to their local environment (Kapoor et al. 2016; Nikodemova et al. 2014); thus assessing microglia number and specific morphology in other respiratory regions of the brain in normoxia and hypoxia could provide further insight into their roles in VAH and central respiratory control.

*Critique of methods.* We used minocycline as a pharmacological tool to inhibit microglia based on previous published research taking the same approach (Blackbeard et al. 2007; Lorea-Hernández et al. 2016; MacFarlane et al. 2016; Tadmouri et al. 2014). However, a recent review of the literature on minocycline and microglia (Möller et al. 2016) considers the general anti-inflammatory effects of this antibiotic and the challenges in determining whether physiological responses to minocycline result from molecular mechanisms of such anti-inflammatory effects independent of microglia. Although microglia activation can lead to increased cytokine production and inflammatory responses, inflammatory cytokines can stimulate microglia as well (Hanisch and Kettenmann 2007). This reciprocal effect is particularly relevant to consider for our experiments because we know that nonsteroidal anti-inflammatory drugs (e.g., ibuprofen) can block increases in the HVR with chronic hypoxia (Basaran et al. 2016; Popa et al. 2011) and minocycline blocks increases in mRNA for inflammatory cytokines interleukin-6 and TNF- $\alpha$  (Hocker et al. 2017). Therefore, it is impossible to attribute the effects of minocycline on ventilatory acclimatization to hypoxia to microglia unequivocally. However, the effect of minocycline to block microglial activation is widely supported by the literature, and minocycline is the only pharmacological tool we presently have to block microglia activation in vivo for experiments such as ours. Importantly, Lorea-Hernández et al. (2016) recently studied the effects of various putative microglial activators and inhibitors on neural generation of the respiratory rhythm in vitro and in vivo and found that the effects of minocycline were consistent with an inhibitory effect on microglial activation vs. anti-inflammatory effects on respiratory center neurons. Hence, we need to qualify our conclusions about the effects of minocycline, and a logical next step to determine the role of

microglia in VAH is to use other, more specific, methods to block microglia activation (Elmore et al. 2014).

Another methodological issue that may affect our conclusions is the difference in the methods used to quantify activation of astrocytes and microglia. Astrocyte activation is generally quantified by measuring an increase in GFAP protein expression with immunohistochemistry for GFAP, which is increased in activated astrocytes (Eng and Ghirnikar 1994). Microglia activation, on the other hand, has been quantified by a number of methods, including Iba-1 protein expression (Chen et al. 2012; Ito et al. 2001; Stokes et al. 2013), immunohistochemistry to colocalize Iba-1 with macrophage proteins often expressed during microglia activation such as CD68, CD11b, or CD45 (Perego et al. 2011; Tadmouri et al. 2014; Turtzo et al. 2014), and morphological changes similar to those we used (Fontainhas et al. 2011; Morrison and Filosa 2013). Because we are quantifying activation of two different cell types using two different metrics (protein expression in astrocytes vs. morphological change of microglia), the response times of these two metrics needs to be considered. Changes in GFAP protein expression should occur quickly, however, because GFAP is ~50 kDa in size and could undergo transcription and translation in as quickly as a few minutes. Upregulation of GFAP protein expression has been shown as early as 1 h in both rat tissue (Amaducci et al. 1981) and human blood (Papa et al. 2016). Similarly, microglia begin to retract their processes within 30 min of activation (Rupalla et al. 1998; Stence et al. 2001). The earliest time point in our studies was 1 h, so we conclude that the different methods cannot explain our results. However, further study is warranted.

*Physiological significance.* As discussed above, our data add to the growing evidence for inflammatory signaling and glial cell activation in medullary respiratory centers during sustained hypoxia, and this is important for ventilatory acclimatization to hypoxia (Hocker et al. 2017). We hypothesize that glial activation is an important step in generating inflammatory signals that appear necessary for neural plasticity during acclimatization to hypoxia. Evidence for this includes a significant decrease in the HVR of healthy humans acclimatizing to high altitude when they receive ibuprofen (a nonsteroidal anti-inflammatory drug) from the onset of high-altitude exposure (Basaran et al. 2016). Similarly, ibuprofen administered to rats during chronic hypoxia completely blocks their normal time-dependent increase in HVR and also blocks increased expression of inflammatory cytokine genes (IL-1 $\beta$ , IL-6) in the NTS (Popa et al. 2011). Recently, we observed that minocycline treatment during 24 h of sustained hypoxia blocks increased TNF- $\alpha$  and IL-6 gene expression in the NTS (Hocker et al. 2017). Here we show that the putative effect of minocycline to block microglial activation also blocks ventilatory acclimatization to hypoxia (Fig. 1) although it cannot reverse it (Fig. 2). Microglia activation precedes astrocyte activation in the NTS during CH (Figs. 3 and 4), both of which are blocked by minocycline (Fig. 5), but minocycline has no effect on microglia or astrocytes in the NTS during normoxia (Fig. 5). Taken together, the results support that microglial activation is a signal or source for inflammatory signals that are necessary for plasticity in VAH.

Here we focus on the NTS for glial cell activation because plasticity in this central respiratory center has been shown to be important for VAH (Accorsi-Mendonça et al. 2015; Pamerter

et al. 2014a, 2014b; Tadmouri et al. 2014; Zhang et al. 2009), and such activation is not observed in all parts of the brain (Tadmouri et al. 2014). However, it is not completely clear how hypoxia can uniquely activate glia in the NTS. The carotid body is necessary for VAH also (reviewed by Kumar and Prabhakar 2012) and exhibits increased expression of inflammatory cytokines from resident immune and glomus cells, as well as with macrophage infiltration during chronic hypoxia (Liu et al. 2009, 2011; Porzionato et al. 2013). Such inflammatory responses in the carotid body may affect the CNS also via synaptic transmission at the primary synapse in the NTS. Chronic hypoxia increases NF- $\kappa$ B, in the carotid body, which promotes the transcription of proinflammatory cytokines including IL-1 $\beta$  (Liu et al. 2009). IL-1 $\beta$  can directly affect NTS neurons and modulate breathing patterns (Aleksandrova and Danilova 2010; Jacono et al. 2011), leading to cyclooxygenase-2 (COX-2) production (Samad et al. 2001). It is possible that the effects of ibuprofen (a COX inhibitor) to block VAH (Basaran et al. 2016; Popa et al. 2011) could be working via this pathway, but this remains to be experimentally tested. Alternatively, changes in afferent input to the NTS may activate microglia, gene expression, or inflammatory responses in the NTS in an activity-dependent manner.

Finally, our data support the idea that sequential ordering of glial activation is important for ventilatory acclimatization to hypoxia. We found evidence for activation of microglia preceding that of astrocytes, and, if we blocked microglial activation with minocycline, we blocked both astrocyte activation and VAH. However, if we blocked microglia activation with minocycline after VAH was already established, we could not reverse the VAH. Microglia and astrocytes are capable of producing a wide range of proinflammatory mediators, including the cytokines discussed above, and microglia have tissue-dependent cytokine profiles and response times (Smith et al. 2013). Such tissue- or stimulus-specific differences in the sequence of glial activation and inflammatory signal changes may be important in determining physiological responses. For example, LPS increases cytokines in the carotid body and NTS (Fernández et al. 2008; Gauda et al. 2013), but this decreases carotid body O<sub>2</sub> sensitivity (Zapata et al. 2011) and impairs chemoreflexes (Huxtable et al. 2011). However, sustained hypoxia produces the opposite effects with increased cytokines, O<sub>2</sub> sensitivity, and HVR (Liu et al. 2009; Popa et al. 2011). The potential role of the sequence of glial activation and specific inflammatory signals in explaining these differences remains to be investigated.

#### ACKNOWLEDGMENTS

The authors thank the laboratory of Dr. Tony Yaksh for the kind use of their cryostat.

#### GRANTS

This work was supported by NIH grants RO1 HL-081823, T32 HL098062-04A, and P30 NS047101.

#### DISCLOSURES

No conflicts of interest, financial or otherwise, are declared by the authors.

#### AUTHOR CONTRIBUTIONS

Study design (JAS, FLP); study execution (JAS, TEA, EAM, ZF); data analysis (JAS, FLP); manuscript preparation (JAS, TEA, EAM, FLP).

#### REFERENCES

- Accorsi-Mendonça D, Machado BH. Synaptic transmission of baro- and chemoreceptors afferents in the NTS second order neurons. *Auton Neurosci* 175: 3–8, 2013. doi:10.1016/j.autneu.2012.12.002.
- Accorsi-Mendonça D, Zoccal DB, Bonagamba LG, Machado BH. Glial cells modulate the synaptic transmission of NTS neurons sending projections to ventral medulla of Wistar rats. *Physiol Rep* 1: e00080, 2013. doi:10.1002/phy2.80.
- Accorsi-Mendonça D, Almado CE, Bonagamba LG, Castania JA, Moraes DJ, Machado BH. Enhanced firing in NTS induced by short-term sustained hypoxia is modulated by glia-neuron interaction. *J Neurosci* 35: 6903–6917, 2015. doi:10.1523/JNEUROSCI.4598-14.2015.
- Aleksandrova NP, Danilova GA. Effect of intracerebroventricular injection of interleukin-1-beta on the ventilatory response to hyperoxic hypercapnia. *Eur J Med Res* 15, Suppl 2: 3–6, 2010.
- Allen NJ. Astrocyte regulation of synaptic behavior. *Annu Rev Cell Dev Biol* 30: 439–463, 2014. doi:10.1146/annurev-cellbio-100913-013053.
- Amaducci L, Forno KI, Eng LF. Glial fibrillary acidic protein in cryogenic lesions of the rat brain. *Neurosci Lett* 21: 27–32, 1981. doi:10.1016/0304-3940(81)90052-5.
- Basaran KE, Villongo M, Ho B, Ellis E, Zarndt R, Antonova J, Hopkins SR, Powell FL. Ibuprofen blunts ventilatory acclimatization to sustained hypoxia in humans. *PLoS One* 11: e0146087, 2016. doi:10.1371/journal.pone.0146087.
- Bezzi P, Volterra A. A neuron-glia signalling network in the active brain. *Curr Opin Neurobiol* 11: 387–394, 2001. doi:10.1016/S0959-4388(00)00223-3.
- Blackbeard J, O'Dea KP, Wallace VC, Segerdahl A, Pheby T, Takata M, Field MJ, Rice AS. Quantification of the rat spinal microglial response to peripheral nerve injury as revealed by immunohistochemical image analysis and flow cytometry. *J Neurosci Methods* 164: 207–217, 2007. doi:10.1016/j.jneumeth.2007.04.013.
- Chen Z, Jalabi W, Shpargel KB, Farabaugh KT, Dutta R, Yin X, Kidd GJ, Bergmann CC, Stohlman SA, Trapp BD. Lipopolysaccharide-induced microglial activation and neuroprotection against experimental brain injury is independent of hematogenous TLR4. *J Neurosci* 32: 11706–11715, 2012. doi:10.1523/JNEUROSCI.0730-12.2012.
- Chitravanshi VC, Sapru HN. Chemoreceptor-sensitive neurons in commissural subnucleus of nucleus tractus solitarius of the rat. *Am J Physiol Regul Integr Comp Physiol* 268: R851–R858, 1995.
- Dissing-Olesen L, LeDue JM, Rungta RL, Hefendehl JK, Choi HB, MacVicar BA. Activation of neuronal NMDA receptors triggers transient ATP-mediated microglial process outgrowth. *J Neurosci* 34: 10511–10527, 2014. doi:10.1523/JNEUROSCI.0405-14.2014.
- Donoghue S, Felder RB, Jordan D, Spyer KM. The central projections of carotid baroreceptors and chemoreceptors in the cat: A neurophysiological study. *J Physiol* 347: 397–409, 1984. doi:10.1113/jphysiol.1984.sp015072.
- Drorbaugh JE, Fenn WO. A barometric method for measuring ventilation in newborn infants. *Pediatrics* 16: 81–87, 1955.
- Dwinell MR, Powell FL. Chronic hypoxia enhances the phrenic nerve response to arterial chemoreceptor stimulation in anesthetized rats. *J Appl Physiol* 87: 817–823, 1999.
- Elmore MR, Najafi AR, Koike MA, Dagher NN, Spangenberg EE, Rice RA, Kitazawa M, Matusow B, Nguyen H, West BL, Green KN. Colony-stimulating factor 1 receptor signaling is necessary for microglia viability, unmasking a microglia progenitor cell in the adult brain. *Neuron* 82: 380–397, 2014. doi:10.1016/j.neuron.2014.02.040.
- Eng LF, Ghirnikar RS. GFAP and astrogliosis. *Brain Pathol* 4: 229–237, 1994. doi:10.1111/j.1750-3639.1994.tb00838.x.
- Erlichman JS, Leiter JC, Gourine AV. ATP, glia and central respiratory control. *Respir Physiol Neurobiol* 173: 305–311, 2010. doi:10.1016/j.resp.2010.06.009.
- Fernández R, González S, Rey S, Cortés PP, Maisey KR, Reyes EP, Larrain C, Zapata P. Lipopolysaccharide-induced carotid body inflammation in cats: Functional manifestations, histopathology and involvement of tumour necrosis factor-alpha. *Exp Physiol* 93: 892–907, 2008. doi:10.1113/expphysiol.2008.041152.
- Fontainhas AM, Wang M, Liang KJ, Chen S, Mettu P, Damani M, Fariss RN, Li W, Wong WT. Microglial morphology and dynamic behavior is regulated by ionotropic glutamatergic and GABAergic neurotransmission. *PLoS One* 6: e15973, 2011. doi:10.1371/journal.pone.0015973.
- Fukushi I, Takeda K, Yokota S, Hasebe Y, Sato Y, Pokorski M, Horiuchi J, Okada Y. Effects of arundic acid, an astrocytic modulator, on the cerebral

- and respiratory functions in severe hypoxia. *Respir Physiol Neurobiol* 226: 24–29, 2016. doi:10.1016/j.resp.2015.11.011.
- Funk GD, Rajani V, Alvares TS, Revill AL, Zhang Y, Chu NY, Biancardi V, Linhares-Taxini C, Katzell A, Reklow R.** Neuroglia and their roles in central respiratory control: An overview. *Comp Biochem Physiol A Mol Integr Physiol* 186: 83–95, 2015. doi:10.1016/j.cbpa.2015.01.010.
- Gauda EB, Shirahata M, Mason A, Pichard LE, Kostuk EW, Chavez-Valdez R.** Inflammation in the carotid body during development and its contribution to apnea of prematurity. *Respir Physiol Neurobiol* 185: 120–131, 2013. doi:10.1016/j.resp.2012.08.005.
- González-Scarano F, Baltuch G.** Microglia as mediators of inflammatory and degenerative diseases. *Annu Rev Neurosci* 22: 219–240, 1999. doi:10.1146/annurev.neuro.22.1.219.
- Gourine AV, Kasymov V, Marina N, Tang F, Figueiredo MF, Lane S, Teschemacher AG, Spyer KM, Deisseroth K, Kasparov S.** Astrocytes control breathing through pH-dependent release of ATP. *Science* 329: 571–575, 2010. doi:10.1126/science.1190721.
- Hanisch UK, Kettenmann H.** Microglia: Active sensor and versatile effector cells in the normal and pathologic brain. *Nat Neurosci* 10: 1387–1394, 2007. doi:10.1038/nn1997.
- Hocker AD, Stokes JA, Powell FL, Huxtable AG.** The impact of inflammation on respiratory plasticity. *Exp Neurol* 287: 243–253, 2017. doi:10.1016/j.expneurol.2016.07.022.
- Hülsmann S, Oku Y, Zhang W, Richter DW.** Metabolic coupling between glia and neurons is necessary for maintaining respiratory activity in transverse medullary slices of neonatal mouse. *Eur J Neurosci* 12: 856–862, 2000. doi:10.1046/j.1460-9568.2000.00973.x.
- Huxtable AG, Zwicker JD, Alvares TS, Ruangkittisakul A, Fang X, Hahn LB, Posse de Chaves E, Baker GB, Ballanyi K, Funk GD.** Glia contribute to the purinergic modulation of inspiratory rhythm-generating networks. *J Neurosci* 30: 3947–3958, 2010. doi:10.1523/JNEUROSCI.6027-09.2010.
- Huxtable AG, Vinit S, Windelborn JA, Crader SM, Guenther CH, Watters JJ, Mitchell GS.** Systemic inflammation impairs respiratory chemoreflexes and plasticity. *Respir Physiol Neurobiol* 178: 482–489, 2011. doi:10.1016/j.resp.2011.06.017.
- Ito D, Tanaka K, Suzuki S, Dembo T, Fukuuchi Y.** Enhanced expression of Iba1, ionized calcium-binding adapter molecule 1, after transient focal cerebral ischemia in rat brain. *Stroke* 32: 1208–1215, 2001. doi:10.1161/01.STR.32.5.1208.
- Jacomo FJ, Mayer CA, Hsieh YH, Wilson CG, Dick TE.** Lung and brainstem cytokine levels are associated with breathing pattern changes in a rodent model of acute lung injury. *Respir Physiol Neurobiol* 178: 429–438, 2011. doi:10.1016/j.resp.2011.04.022.
- Ji K, Akgul G, Wollmuth LP, Tsirka SE.** Microglia actively regulate the number of functional synapses. *PLoS One* 8: e56293, 2013. doi:10.1371/journal.pone.0056293.
- Kapoor K, Bhandare AM, Mohammed S, Farnham MM, Pilowsky PM.** Microglial number is related to the number of tyrosine hydroxylase neurons in SHR and normotensive rats. *Auton Neurosci* 198: 10–18, 2016. doi:10.1016/j.autneu.2016.05.005.
- Kettenmann H, Kirchhoff F, Verkhratsky A.** Microglia: New roles for the synaptic stripper. *Neuron* 77: 10–18, 2013. doi:10.1016/j.neuron.2012.12.023.
- Kreutzberg GW.** Microglia: A sensor for pathological events in the CNS. *Trends Neurosci* 19: 312–318, 1996. doi:10.1016/0166-2236(96)10049-7.
- Kumar P, Prabhakar NR.** Peripheral chemoreceptors: Function and plasticity of the carotid body. *Compr Physiol* 2: 141–219, 2012. doi:10.1002/cphy.c100069.
- Lawson LJ, Perry VH, Dri P, Gordon S.** Heterogeneity in the distribution and morphology of microglia in the normal adult mouse brain. *Neuroscience* 39: 151–170, 1990. doi:10.1016/0306-4522(90)90229-W.
- Lin LH, Moore SA, Jones SY, McGlashan J, Talman WT.** Astrocytes in the rat nucleus tractus solitarius are critical for cardiovascular reflex control. *J Neurosci* 33: 18608–18617, 2013. doi:10.1523/JNEUROSCI.3257-13.2013.
- Liu X, He L, Stensaas L, Dinger B, Fidone S.** Adaptation to chronic hypoxia involves immune cell invasion and increased expression of inflammatory cytokines in rat carotid body. *Am J Physiol Lung Cell Mol Physiol* 296: L158–L166, 2009. doi:10.1152/ajplung.90383.2008.
- Liu X, He L, Dinger B, Gonzalez C, Stensaas L, Fidone S.** A chronic pain: Inflammation-dependent chemoreceptor adaptation in rat carotid body. *Respir Physiol Neurobiol* 178: 362–369, 2011. doi:10.1016/j.resp.2011.03.006.
- Lorea-Hernández JJ, Morales T, Rivera-Angulo AJ, Alcántara-González D, Peña-Ortega F.** Microglia modulate respiratory rhythm generation and autoresuscitation. *Glia* 64: 603–619, 2016. doi:10.1002/glia.22951.
- MacFarlane PM, Mayer CA, Litvin DG.** Microglia modulate brainstem serotonergic expression following neonatal sustained hypoxia exposure: Implications for sudden infant death syndrome. *J Physiol* 594: 3079–3094, 2016. doi:10.1113/JP271845.
- Miffiin SW.** Arterial chemoreceptor input to nucleus tractus solitarius. *Am J Physiol Regul Integr Comp Physiol* 263: R368–R375, 1992.
- Möller T, Bard F, Bhattacharya A, Biber K, Campbell B, Dale E, Eder C, Gan L, Garden GA, Hughes ZA, Pearse DD, Staal RG, Sayed FA, Wes PD, Boddeke HW.** Critical data-based re-evaluation of minocycline as a putative specific microglia inhibitor. *Glia* 64: 1788–1794, 2016. doi:10.1002/glia.23007.
- Morrison HW, Filosa JA.** A quantitative spatiotemporal analysis of microglia morphology during ischemic stroke and reperfusion. *J Neuroinflammation* 10: 4, 2013. doi:10.1186/1742-2094-10-4.
- Nikodemova M, Small AL, Smith SM, Mitchell GS, Watters JJ.** Spinal but not cortical microglia acquire an atypical phenotype with high VEGF, galectin-3 and osteopontin, and blunted inflammatory responses in ALS rats. *Neurobiol Dis* 69: 43–53, 2014. doi:10.1016/j.nbd.2013.11.009.
- Nimmerjahn A, Kirchhoff F, Helmchen F.** Resting microglial cells are highly dynamic surveillants of brain parenchyma in vivo. *Science* 308: 1314–1318, 2005. doi:10.1126/science.1110647.
- Pamenter ME, Powell FL.** Time domains of the hypoxic ventilatory response and their molecular basis. *Compr Physiol* 6: 1345–1385, 2016. doi:10.1002/cphy.c150026.
- Pamenter ME, Carr JA, Go A, Fu Z, Reid SG, Powell FL.** Glutamate receptors in the nucleus tractus solitarius contribute to ventilatory acclimatization to hypoxia in rat. *J Physiol* 592: 1839–1856, 2014a. doi:10.1113/jphysiol.2013.268706.
- Pamenter ME, Nguyen J, Carr JA, Powell FL.** The effect of combined glutamate receptor blockade in the NTS on the hypoxic ventilatory response in awake rats differs from the effect of individual glutamate receptor blockade. *Physiol Rep* 2: e12092, 2014b. doi:10.14814/phy2.12092.
- Panatier A, Vallée J, Haber M, Murai KK, Lacaille JC, Robitaille R.** Astrocytes are endogenous regulators of basal transmission at central synapses. *Cell* 146: 785–798, 2011. doi:10.1016/j.cell.2011.07.022.
- Papa L, Brophy GM, Welch RD, Lewis LM, Braga CF, Tan CN, Ameli NJ, Lopez MA, Haeussler CA, Mendez Giordano DI, Silvestri S, Giordano P, Weber KD, Hill-Pryor C, Hack DC.** Time course and diagnostic accuracy of glial and neuronal blood biomarkers GFAP and UCH-L1 in a large cohort of trauma patients with and without mild traumatic brain injury. *JAMA Neurol* 73: 551–560, 2016. doi:10.1001/jamaneurol.2016.0039.
- Pascual O, Ben Achour S, Rostaing P, Triller A, Bessis A.** Microglia activation triggers astrocyte-mediated modulation of excitatory neurotransmission. *Proc Natl Acad Sci USA* 109: E197–E205, 2012. doi:10.1073/pnas.1111098109.
- Perego C, Fumagalli S, De Simoni MG.** Temporal pattern of expression and colocalization of microglia/macrophage phenotype markers following brain ischemic injury in mice. *J Neuroinflammation* 8: 174, 2011. doi:10.1186/1742-2094-8-174.
- Popa D, Fu Z, Go A, Powell FL.** Ibuprofen blocks time-dependent increases in hypoxic ventilation in rats. *Respir Physiol Neurobiol* 178: 381–386, 2011. doi:10.1016/j.resp.2011.03.024.
- Porzionato A, Macchi V, De Caro R, Di Giulio C.** Inflammatory and immunomodulatory mechanisms in the carotid body. *Respir Physiol Neurobiol* 187: 31–40, 2013. doi:10.1016/j.resp.2013.02.017.
- Powell FL, Milsom WK, Mitchell GS.** Time domains of the hypoxic ventilatory response. *Respir Physiol* 112: 123–134, 1998. doi:10.1016/S0034-5687(98)00026-7.
- Reid SG, Powell FL.** Effects of chronic hypoxia on MK-801-induced changes in the acute hypoxic ventilatory response. *J Appl Physiol* 99: 2108–2114, 2005. doi:10.1152/jappphysiol.01205.2004.
- Roy A, Jana A, Yatish K, Freidt MB, Fung YK, Martinson JA, Pahan K.** Reactive oxygen species up-regulate CD11b in microglia via nitric oxide: Implications for neurodegenerative diseases. *Free Radic Biol Med* 45: 686–699, 2008. doi:10.1016/j.freeradbiomed.2008.05.026.
- Rupalla K, Allegrini PR, Sauer D, Wiessner C.** Time course of microglia activation and apoptosis in various brain regions after permanent focal cerebral ischemia in mice. *Acta Neuropathol* 96: 172–178, 1998. doi:10.1007/s004010050878.
- Samad TA, Moore KA, Sapirstein A, Billet S, Allchorne A, Poole S, Bonventre JV, Woolf CJ.** Interleukin-1beta-mediated induction of Cox-2 in the CNS contributes to inflammatory pain hypersensitivity. *Nature* 410: 471–475, 2001. doi:10.1038/35068566.

- Smith SM, Friedle SA, Watters JJ.** Chronic intermittent hypoxia exerts CNS region-specific effects on rat microglial inflammatory and TLR4 gene expression. *PLoS One* 8: e81584, 2013. doi:[10.1371/journal.pone.0081584](https://doi.org/10.1371/journal.pone.0081584).
- Stence N, Waite M, Dailey ME.** Dynamics of microglial activation: a confocal time-lapse analysis in hippocampal slices. *Glia* 33: 256–266, 2001. doi:[10.1002/1098-1136\(200103\)33:3<256::AID-GLIA1024>3.0.CO;2-J](https://doi.org/10.1002/1098-1136(200103)33:3<256::AID-GLIA1024>3.0.CO;2-J).
- Stokes JA, Cheung J, Eddinger K, Corr M, Yaksh TL.** Toll-like receptor signaling adapter proteins govern spread of neuropathic pain and recovery following nerve injury in male mice. *J Neuroinflammation* 10: 148, 2013. doi:[10.1186/1742-2094-10-148](https://doi.org/10.1186/1742-2094-10-148).
- Tadmouri A, Champagnat J, Morin-Surun MP.** Activation of microglia and astrocytes in the nucleus tractus solitarius during ventilatory acclimatization to 10% hypoxia in unanesthetized mice. *J Neurosci Res* 92: 627–633, 2014. doi:[10.1002/jnr.23336](https://doi.org/10.1002/jnr.23336).
- Tremblay ME, Stevens B, Sierra A, Wake H, Bessis A, Nimmerjahn A.** The role of microglia in the healthy brain. *J Neurosci* 31: 16064–16069, 2011. doi:[10.1523/JNEUROSCI.4158-11.2011](https://doi.org/10.1523/JNEUROSCI.4158-11.2011).
- Turtzo LC, Lescher J, Janes L, Dean DD, Budde MD, Frank JA.** Macrophagic and microglial responses after focal traumatic brain injury in the female rat. *J Neuroinflammation* 11: 82, 2014. doi:[10.1186/1742-2094-11-82](https://doi.org/10.1186/1742-2094-11-82).
- Vesce S, Bezzi P, Volterra A.** The active role of astrocytes in synaptic transmission. *Cell Mol Life Sci* 56: 991–1000, 1999. doi:[10.1007/s000180050488](https://doi.org/10.1007/s000180050488).
- Wilkinson KA, Huey K, Dinger B, He L, Fidone S, Powell FL.** Chronic hypoxia increases the gain of the hypoxic ventilatory response by a mechanism in the central nervous system. *J Appl Physiol* 109: 424–430, 2010. doi:[10.1152/jappphysiol.01311.2009](https://doi.org/10.1152/jappphysiol.01311.2009).
- Zapata P, Larraín C, Reyes P, Fernández R.** Immunosensory signalling by carotid body chemoreceptors. *Respir Physiol Neurobiol* 178: 370–374, 2011. doi:[10.1016/j.resp.2011.03.025](https://doi.org/10.1016/j.resp.2011.03.025).
- Zhang W, Carreño FR, Cunningham JT, Mifflin SW.** Chronic sustained hypoxia enhances both evoked EPSCs and norepinephrine inhibition of glutamatergic afferent inputs in the nucleus of the solitary tract. *J Neurosci* 29: 3093–3102, 2009. doi:[10.1523/JNEUROSCI.2648-08.2009](https://doi.org/10.1523/JNEUROSCI.2648-08.2009).

